

Fluctuating diamagnetism in underdoped high-temperature superconductors

Alain Sewer^{1,2} and Hans Beck²

¹*Institut Romand de Recherche Numérique en Physique des Matériaux (IRRMA), EPFL, 1015 Lausanne, Switzerland*

²*Institut de Physique, Université de Neuchâtel, 2000 Neuchâtel, Switzerland*

(Received 18 December 2000; published 12 June 2001)

The fluctuation-induced diamagnetism of underdoped high-temperature superconductors is studied in the framework of the Lawrence-Doniach model. By taking into account the fluctuations of the phase of the order parameter only, the latter reduces to a layered XY model describing a liquid of vortices that can be either thermally excited or induced by the external magnetic field. The diamagnetic response is given by a current-current correlation function that is evaluated using the Coulomb-gas analogy. Our results are then applied to recent measurements of fluctuation diamagnetism in underdoped $\text{YBa}_2\text{Cu}_3\text{O}_{6.67}$. They make possible the understanding of both the observed anomalous temperature dependence of the zero-field susceptibility and the two distinct regimes appearing in the magnetic-field dependence of the magnetization.

DOI: 10.1103/PhysRevB.64.014510

PACS number(s): 74.20.De, 74.25.Ha, 74.40.+k

I. INTRODUCTION

Owing to their short coherence length, high-temperature superconductors show marked deviations from the mean-field behavior that describes rather well the behavior of conventional superconductors. The underdoped regime of the various cuprates is particularly interesting, given their pronounced anisotropy and the low density of charge carriers. In this region of the phase diagram, fluctuations are strongly enhanced and are manifest already well above the critical temperature T_c . This fluctuation regime gives rise to various unusual phenomena,¹ such as an anomalous temperature dependence of the Knight shift, NMR relaxation rate and electrical conductivity, an anomalous frequency dependence of infrared conductivity, as well as the formation of a pseudogap in the electronic density of states. Close to T_c it also allows to see true critical behavior in quantities such as the specific heat² or thermal expansion.³

In the present work, we specifically address the temperature and field dependence of the diamagnetic susceptibility χ of strongly anisotropic high-temperature superconductors above T_c . The influence of fluctuations on χ has been studied long ago in the framework of a Landau-Ginzburg model, taking into account Gaussian fluctuations of the order parameter above the critical temperature.⁴ More-refined calculations based on the Lawrence-Doniach model have taken into account the lattice structure.⁵ Recent measurements⁶ have shown that the Gaussian approximation can indeed well describe the diamagnetic fluctuations in optimally doped $\text{YBa}_2\text{Cu}_3\text{O}_7$ (YBCO), whereas underdoped specimens of the same compound, such as $\text{YBa}_2\text{Cu}_3\text{O}_{6.67}$, show dramatic deviations from this behavior. The fluctuation region where the zero-field orbital susceptibility shows appreciable values extends over a much larger temperature range than in the optimally doped system. Moreover, the field dependence of the magnetization shows a much more pronounced crossover between low and high fields than what would have been expected from Gaussian fluctuations.

We base our calculations on an anisotropic Lawrence-Doniach (LD) functional, involving the superconducting order-parameter field Δ in the presence of a vector potential

that describes a homogeneous magnetic field perpendicular to the lattice planes. Rather than considering Gaussian fluctuations, we assume a ‘‘precursor regime’’ in which the amplitude of Δ has already acquired a nonzero average value whereas its phase is subject to strong fluctuations inhibiting long-range superconducting order. In this context the LD functional reduces to an anisotropic layered XY model. The relevant thermal excitations of such a system are the phase-field singularities that manifest themselves as vortices and antivortices in two dimensions (2D) and as vortex loops in 3D. The applied magnetic field also acts on the phases by inducing vortex lines crossing the sample from one end to the other. The diamagnetic susceptibility, expressed in the usual way by a current-current correlation function, is then related to the positional correlation function of the vortex-line elements, the static structure factor $S(\mathbf{q})$. We model $S(\mathbf{q})$ in a simple way by using various known results obtained either by analytic considerations based on the Coulomb-gas analogy or by Monte Carlo (MC) simulations of the anisotropic 3D XY model. Then we arrive at explicit expressions for the zero-field susceptibility $\chi(T)$ and the temperature and field-dependent magnetization $M(T, B)$. They contain several material-dependent parameters that are estimated by comparing with the experimental data on underdoped YBaCuO from Ref. 6.

This procedure unravels three main features. First, the density of the vortex-line elements contributing to the diamagnetic response (those that are oriented in z direction, i.e., parallel to the applied field) is thermally activated with a value of the activation energy that is compatible with what is found in the above mentioned MC simulations. Second, in the temperature range covered by the experiments, the value of the anisotropy shows that the positions of the vortex-line elements fluctuate strongly from one layer to the other. This points to a rather weak effective coupling between layers, which is compatible with the fact of being above the vortex melting and the ‘‘vortex decoupling’’ line. Finally the rather sharp crossover of the magnetization $M(T, B)$ as a function of B points to a subtle interplay between thermally excited vortex loops and field-induced vortex lines.

These observations allow for the following conclusions.

(i) The experiments in Ref. 6 can be much better accounted for by phase excitations than by Gaussian fluctuations of the pairing field. This is particularly manifest in the activated T dependence of the susceptibility, but also in the existence of two field regimes with quite different behaviors of the magnetization. In this context we have, however, to admit that the very sharp crossover between these two regimes observed in the experiment may also be due to sample inhomogeneities as it was suggested in the experimental papers.⁶

(ii) Except for the data taken close to the zero-field critical temperature, the diamagnetic response of the underdoped compound presented in Ref. 6 seems to be “precritical,” in the sense that the relevant lengths in the lattice planes as well as in the perpendicular direction do not show any true critical (i.e., singular) behavior (which would be supposed to belong to the 3D XY universality class³).

In Sec. II we develop the theoretical formalism that allows to express $\chi(T)$ and $M(T, B)$ in terms of the vortex-line structure factor, and in Sec. III we compare our theoretical results with the data presented in Ref. 6 for underdoped YBCO, thereby extracting the free parameters from the experimental curves. A summary is presented in Sec. IV.

II. DIAMAGNETIC RESPONSE

We discuss the orbital magnetic response of an underdoped superconductor in the London approximation to the LD model, i.e., in the framework of an 3D anisotropic layered XY model in which the phase θ of the superconducting order parameter Δ is coupled to the vector potential \mathbf{A}_{\parallel} describing a homogeneous magnetic field \mathbf{B} perpendicular to the lattice planes (we restrict ourselves to temperatures $T > T_c$ where the Meissner effect is absent, identifying thus the external and the effective internal vector potential),

$$\mathcal{H}[\theta] = \frac{1}{2a^2d} \sum_n \int d^2r \left\{ J_{\parallel} a^2 \left[\nabla_{\parallel} \theta_n - \frac{2\pi}{\Phi_0} \mathbf{A}_{\parallel} \right]^2 + J_{\perp} [1 - \cos(\theta_n - \theta_{n+1})] \right\}. \quad (1)$$

Here a is the lattice constant in the planes whereas d denotes the distance between two layers. J_{\parallel} and J_{\perp} are the respective phase couplings. Their ratio

$$\gamma^2 = \frac{J_{\parallel}}{J_{\perp}} > 1 \quad (2)$$

determines the anisotropy of the system. The XY Hamiltonian can be obtained starting from a LD functional for the complex superconducting pairing field Δ by keeping the amplitude of the latter constant (London approximation). This is a current strategy⁷ based on the assumption that the various precursor phenomena, observed in underdoped cuprates between T_c and some higher temperature T^* and mentioned in the Introduction, are essentially due to fluctuations of the phase of Δ whereas its amplitude $|\Delta|$ maintains a finite mean value. Moreover, these materials exhibit a layered structure that is specifically taken into account by the Lawrence-

Doniach approach. Expression (1) is a partial continuum version of the discrete-3D XY model, the Josephson coupling $1 - \cos(\theta_i - \theta_j)$ between neighboring lattice sites in a given layer having been replaced by the phase gradient.

The orbital magnetic response Λ in a finite external field is obtained by adding a small perturbation to the applied vector potential

$$\mathbf{A}_{\parallel} \mapsto \mathbf{A}_{\parallel} + \delta \mathbf{A}_{\parallel} \quad (3)$$

and by calculating the second derivative of the free energy with respect to the perturbing field $\delta \mathbf{A}_{\parallel}$. The magnetic susceptibility $\chi(T, B)$ is then given by

$$\chi = \lim_{q \rightarrow 0} \frac{\Lambda(\mathbf{q})}{q^2} \quad (4)$$

with

$$\Lambda(\mathbf{q}) = \frac{J_{\parallel}}{d} \left(\frac{2\pi}{\Phi_0} \right)^2 \left[\frac{J_{\parallel}}{k_B T} C(\mathbf{q}) - 1 \right]. \quad (5)$$

The second term of Eq. (5) is the diamagnetic response, whereas the first term involves the current-current correlation function

$$C(\mathbf{q}) = \frac{1}{L^2} \sum_{n, n'} \int d^2\rho d^2\rho' e^{i\mathbf{q} \cdot (\mathbf{r} - \mathbf{r}')} \langle j_x(\mathbf{r}) j_x(\mathbf{r}') \rangle, \quad (6)$$

$$j_x(\mathbf{r}) = \nabla_x \theta_n(\boldsymbol{\rho}) - \frac{2\pi}{\Phi_0} A_{\parallel, x}(\mathbf{r}). \quad (7)$$

Here the coordinate \mathbf{r} means $(\boldsymbol{\rho}, nd)$ and the sample volume is $\Omega = L^2 Nd$ where N is the number of layers. In order to have a finite χ , the limit $C(q \rightarrow 0)$ has to cancel the diamagnetic term. It will be shown below that this is indeed the case in our approach. We have chosen the gauge in which

$$\mathbf{A}_{\parallel}(\mathbf{r}) = (-yB, 0, 0). \quad (8)$$

Thus the relevant wave vector \mathbf{q} has only a y component denoted simply by q .

In order to study the thermodynamic properties of the 3D anisotropic XY model, we first recall that the Berezinskii-Kosterlitz-Thouless transition occurring in the strictly 2D case is best described in terms of vortex and antivortex excitations. Although the 3D XY system shows a “normal” second-order transition, even when it is anisotropic, it has been shown that it is also possible to understand the critical behavior of such a system in terms of vortex excitations, which—for topological reasons—now have to form closed loops or continuous lines crossing the whole system.⁸ The loops are the 3D extension of the planar vortex–antivortex structure whereas the lines arise from the presence of an external magnetic flux penetrating into the sample in the same way as in a type II superconductor below T_c . In the following we will use this vortex picture of the 3D XY model in order to calculate the phase correlation function $C(\mathbf{q})$ that determines the diamagnetic response according to Eq. (6). Since vortex lines are either closed (forming a loop)

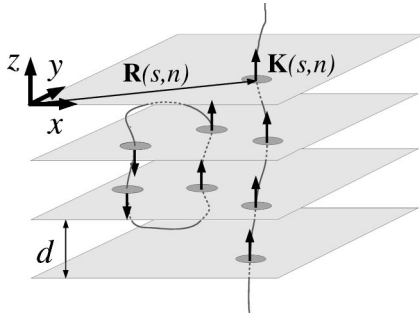


FIG. 1. Schematic representation of a 3D thermally excited vortex loop (left) and of a field-induced vortex line (right). Since in the Lawrence-Doniach approach the phase field is defined only for discrete values of the z coordinate ($z=nd$), one often refers to these structures as “stacks of pancake vortices.” The latter are represented by the gray ellipses whereas the lines linking them are then just guides to the eye.

or extend continuously through the whole sample, we can characterize their structure by labeling each line by an index s and by giving its position $\mathbf{R}(s, n)$ in a given layer n that corresponds to the center of the corresponding “pancake vortex” (see Fig. 1). The x component of the phase gradient created by all the vortex lines is then given by the same expression used in magnetostatics in order to calculate the magnetic field of a system of current loops and lines,

$$\nabla_x \theta_n(\boldsymbol{\rho}) = d \sum_{\alpha, \beta, s, n'} \varepsilon_{x\alpha\beta} \int d^2 \rho' \frac{(r_\alpha - r'_\alpha) K_\beta(s, \mathbf{r}')}{|\mathbf{r} - \mathbf{r}'|^3}. \quad (9)$$

Here $\varepsilon_{\alpha\beta\gamma}$ is the fully antisymmetric tensor of rank 3 and the vector field $\mathbf{K}(s, \mathbf{r}')$ is given by the line element “tangential” to the vortex-line number s at point $\mathbf{r}' = (\boldsymbol{\rho}', n'd)$,

$$\mathbf{K}(s, \mathbf{r}') = t(s, n') \delta(\boldsymbol{\rho}' - \mathbf{R}(s, n')) \hat{\mathbf{z}}, \quad (10)$$

$\hat{\mathbf{z}}$ being the unit vector in the z direction and the sum in Eq. (9) thus runs over all vortex line elements s and layers n . In order to make connection with the (more simple) 2D case, it is useful to attribute a topological number $t(s, n) = \pm 1$ to each vertical-vortex line element. Its sign is chosen such that the product $t(s, n) \hat{\mathbf{z}}$ gives the oriented “tangential” vector of the vortex line at that point [i.e., $t = +1$ (-1), when the line moves upward (downward) with respect to the lattice plane n]. The current correlator (6) is then given by two contributions,

$$C(\mathbf{q}) = \frac{4\pi^2}{L^2 N q^2} \left[S(\mathbf{q}) - \left(\frac{L^2 N B}{\Phi_0} \right)^2 \delta_{\mathbf{q},0} \right]. \quad (11)$$

The first term, stemming from the phase gradient in the current density (7), represents the structure factor of the vortex line elements oriented in z direction, given by

$$S(\mathbf{q}) = \sum_{s, n, s', n'} t(s, n) t(s', n') \langle \exp\{i\mathbf{q} \cdot [\mathbf{R}(s, n) - \mathbf{R}(s', n')]\} \rangle. \quad (12)$$

The other term in Eq. (11) comes from the second (diamagnetic) contribution to the current (7) and represents the total flux going through the system due to the applied field (cross correlations between $\nabla_x \theta$ and $A_{\parallel, x}$ are supposed to vanish due to the disordered structure of the vortex system above the melting temperature). In the Appendix we show that the singular zero-wave vector value of the correlation function $S(\mathbf{q})$ compensates the second contribution to Eq. (11) so that the limit $C(q \rightarrow 0)$ is well behaved. The main problem left is thus to find a suitable form for the regular part of the correlation function $S(\mathbf{q})$.

First, we recall that we are interested in the fluctuation-induced diamagnetism above the zero-field transition temperature T_c , a range in which recent experiments have been carried out.⁶ For a finite field one has thus to deal with a region in the T - B phase diagram lying beyond the different possible transition lines that are discussed in the literature, such as the vortex-melting line and the vortex-decoupling line.^{10,11} Our structure factor $S(\mathbf{q})$ thus has to describe a disordered vortex-liquid system in which strongly “wrinkled” vortex lines and loops^{9,11} go through the sample. We use the following reasoning for obtaining an approximate form of the regular contribution to $S(\mathbf{q})$.

(i) In the extreme limit of totally decoupled layers, each plane would have to be described by a 2D XY model above the critical temperature, which is frustrated when an external magnetic field is applied. Its vortex structure would be the one of a neutral Coulomb gas, more precisely of a mixture of a neutral two-component Coulomb gas (given by an equal number of thermal vortices and antivortices) and of a one-component gas (the field-induced vortices) in a neutralizing background (given by the external flux). In the purely 2D case, the nontrivial part of Eq. (12) thus reduces to

$$\begin{aligned} S_{2D}(\mathbf{q}) &= N \sum_{s, s'} t(s, 0) t(s', 0) \langle \exp\{i\mathbf{q} \cdot [\mathbf{R}(s, 0) - \mathbf{R}(s', 0)]\} \rangle \\ &= NL^2 n_V S_C(\mathbf{q}). \end{aligned} \quad (13)$$

Here we represented the positional structure factor involving a sum over all vortex and antivortex positions by the Coulomb-gas structure factor $S_C(\mathbf{q})$. We use the following approximate form¹²

$$S_C(\mathbf{q}) = \frac{q^2}{q^2 + 2\pi n_V q_V^2 / k_B T}, \quad (14)$$

where n_V is the areal vortex density and the “charge” q_V of each vortex is related to the in-plane phase coupling J_{\parallel} by¹³

$$q_V^2 = 2\pi J_{\parallel}. \quad (15)$$

The expression (14) yields the correct limiting behavior of $S_C(\mathbf{q})$ for $q \rightarrow 0$ and should be valid for temperatures not too close to T_c . Inserting expression (14) into Eq. (11) gives a similar form of the current-current correlation function $C(\mathbf{q})$ as used by Kwon and Dorsey.¹⁴

(ii) For a strong anisotropy and for the considered temperature range the effective interlayer coupling will be very weak. For evaluating expression (12), we split the double

sum over n and n' into two parts. In the first part, we take n equal to n' that yields a 2D-problem analogous to the one treated above. The corresponding contribution to Eq. (12) is therefore similar to the structure factor of point vortices in a single XY plane,

$$S_1(\mathbf{q}) = NL^2 n_V S_C(\mathbf{q}), \quad (16)$$

where n_V is now the areal density of *vertical* vortex-line elements. The second part $S_2(\mathbf{q})$ of the double sum in Eq. (12) contains n and n' involving different layers. Here we use the fact that in the considered temperature range, the vortex loops and also the field-induced lines have a very irregular shape. Indeed, the region in the T - B plane we are interested in lies above any lattice layer decoupling line.¹⁰ This fact is formulated in Ref. 7, by indicating a T domain

$$\frac{|T - T_c|}{T_c} > \gamma^{1/\nu}, \quad (17)$$

with an XY exponent $\nu \approx 0.6$, for which the lattice planes are practically decoupled. Therefore only those ones that are close enough to another (in a sense to be specified below) are correlated and will contribute to $S_2(\mathbf{q})$. We first expand formally in expression (12) the position $\mathbf{R}(s', n')$ of a vortex line s' in layer n' with respect to its value in layer n . This gives

$$S_2(\mathbf{q}) = \sum_{s, s', n, n' \neq n} t(s, n) t(s', n') \langle \exp\{i\mathbf{q} \cdot [\mathbf{R}(s, n) - \mathbf{R}(s', n)]\} \exp\{-i\mathbf{q} \cdot \mathbf{u}(s', n - n')\} \rangle. \quad (18)$$

Then we split the average bracket of Eq. (18) and factor out from the sum over n' the first exponential that pertains to a given layer n as well as the topological numbers $t(s', n')$ that are equal to $t(s', n)$ for neighboring layers n and n' . This yields the previous result (16). We are then left with correlations between the positions \mathbf{R} of a single vortex line s' in layer n' and in layer $n \neq n'$. Assuming that such correlations are the same for all vortex lines s' and extend only over a distance $\xi_3 = n_3 d$, we obtain

$$S_2(\mathbf{q}) = 2 S_1(\mathbf{q}) \sum_{n=1}^{n_3} \langle e^{-i\mathbf{q} \cdot \mathbf{u}(n)} \rangle \equiv 2 S_1(\mathbf{q}) X(\mathbf{q}). \quad (19)$$

Here $\mathbf{u}(n)$ is the deviation of a given line or loop from a straight line along the z direction. The factor 2 comes from the fact that the sums over $n < n'$ and $n > n'$ have been reduced to one such sum in Eq. (19). Assuming that the vortex lines behave like harmonic strings with an effective stiffness given approximately by $\lambda \approx J_\perp / d = J_\parallel / d \gamma^2$, one finds

$$X(\mathbf{q}) \approx \sum_{n=1}^{n_3} \exp\left[-\frac{1}{2} q^2 \langle \mathbf{u}^2(n) \rangle\right] = \frac{1 - \exp(-k_B T n_3 d q^2 / 4\lambda)}{\exp(k_B T d q^2 / 4\lambda) - 1}. \quad (20)$$

Here we used the relation $\langle \mathbf{u}^2(n) \rangle = \frac{1}{2} (k_B T / \lambda) n d$ applying for harmonic deformations and yielding a geometric series. The final result for the regular part of $C(\mathbf{q})$ in Eq. (11) then takes the form

$$C(\mathbf{q}) = \frac{4\pi^2}{q^2} n_V S_C(\mathbf{q}) [1 + 2X(\mathbf{q})]. \quad (21)$$

In order to evaluate χ according to Eq. (4), we have to expand C in powers of q . First, the above-mentioned cancellation of $C(q=0)$ in Eq. (5) with the (first) diamagnetic contribution is fulfilled, provided that the effective charge of the Coulomb-gas structure factor is chosen to be

$$q_V^2 = 2\pi J_\parallel (1 + 2n_3), \quad (22)$$

which is a reasonable generalization of the purely 2D result (15), taking into account the fact that the ‘‘charges’’ are now vortex lines elements correlated over a distance $\sim n_3 d$ along the z direction. The cancellation of the $q=0$ term in Eq. (5) makes the limit (4) finite and guarantees that the phase system of the superconductor has no stiffness above the critical temperature by making the limit (4) finite. Evaluating the latter leads directly to the final result for the bulk susceptibility χ (per unit volume) that reads

$$\chi = -\frac{1}{(1 + 2n_3)d} \frac{k_B T}{\Phi_0^2} \left[\frac{1}{n_V} + (\pi\gamma)^2 n_3 (1 + n_3) d^2 \right]. \quad (23)$$

Expression (23) will be used in the following section for interpreting the experimental data (low-field susceptibility and field dependence of the magnetization) obtained on underdoped YBCO.⁶

III. ANALYSIS OF EXPERIMENTAL MAGNETIZATION AND SUSCEPTIBILITY DATA

In order to apply our theoretical results to underdoped YBCO, we use the following (approximate) values for the lattice parameters : $a = 4 \text{ \AA}$ and $d = 12 \text{ \AA}$. Moreover, the molar quantities like those reported in Ref. 6 are obtained by multiplying expression (23) by the molar volume $\Omega_M = \mathcal{N}_A a^2 d = 115 \text{ cm}^3$ and by a reduction factor λ that accounts for the fact that in the materials we are interested in only a fraction of the unit-cell volume actually carries the current densities and thus contributes to the diamagnetic response.

A. Low-field susceptibility

The susceptibility data of Ref. 6, for a very low applied field of 0.02 T, cover the range from $T = 63 \text{ K}$, which is just above the zero-field transition temperature, to $T = 110 \text{ K}$. Above $T = 80 \text{ K}$ the diamagnetic susceptibility χ is essentially equal to zero, a background consisting of spin susceptibility and free-electron orbital diamagnetism having been subtracted. For zero applied field, our expression (23) for χ contains several yet-undetermined parameters: the areal density n_V of vertical vortex line elements that are thermally

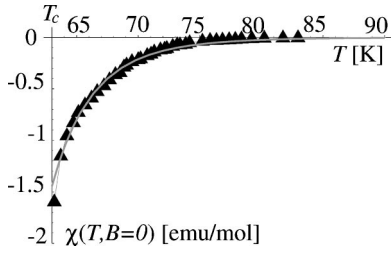


FIG. 2. Zero-field susceptibility $\chi(T, B=0)$: the triangles (\blacktriangle) are the experimental data from Ref. 6 and the full line is the best fit of the theoretical expression (23) assuming the activated behavior (25).

excited, the correlation length $n_3 d$, and the anisotropy γ . We mention that the subsequent analysis of the temperature and field-dependent magnetization will show that the second term of Eq. (23) is irrelevant at low fields. Therefore the value of γ is unimportant and the dominant contribution to $\chi(T, B \rightarrow 0)$ is given by in-plane correlations of the thermal-vortex loop elements. Figure 2, in which the data of Ref. 6 are reproduced with our expression (23), shows that the observed zero-field diamagnetic susceptibility is almost perfectly fitted by

$$\chi(T, B=0) = C \exp\left(\frac{E_0}{k_B T}\right), \quad (24)$$

with $E_0/k_B T_c \approx 22$. This means that the quantity n_V must be temperature dependent and obey a thermally activated behavior

$$n_V = n_0 \exp\left(-\frac{E_0}{k_B T}\right), \quad (25)$$

with the factor $n_0 \sim 10^4/a^2$. The number of vortex excitations in the XY model is indeed known to show an activated T dependence. In 2D this has recently been confirmed¹⁷ and various authors find the same result in 3D^{18–20} using numerical studies. In the first case the activation energy is roughly given by $E_0 \sim 10 k_B T_c$.¹⁷ Simulations for the anisotropic 3D case yield values that are somewhat larger¹⁸ and that depend on the structure of the corresponding loop,^{19–25} getting larger the more planes are crossed. In a strongly anisotropic 3D XY system, most of the thermal loops existing up to the critical temperature consist of elements parallel to the lattice planes.^{8,20,22,24,25} Loop segments perpendicular to the planes only begin to be formed above T_c . Thus the activated form attributed to the vortex-line density n_V in Eq. (25) can be seen as a measure for the rapidly increasing number of loops crossing two planes or even more. Such loops contain at least two line segments perpendicular to the planes, the rest being between two planes. This 3D structure may explain the relatively large value of the activation energy E_0 found above. The latter is also compatible with an explicit expression for the loop self-energy proposed in Ref. 7 assuming that the total length of the loop segments oriented in z direction is on the order of two interplanar distances, the rest of the loop being oriented parallel to the lattice planes. The value of E_0 further suggests that the quantity $n_3 d$ measuring the exten-

sion of the correlations of the vortex structure along the z direction must be of the order of a few lattice distance d (we will take $n_3 = 2$ in the following). This provides an *a posteriori* justification for the assumptions we made when deriving Eq. (21). Finally we note that the fact that the diamagnetic response is associated with loops containing line elements parallel to the z direction directly follows from the magnetostatics: the vertical loop elements are generated by currents flowing perpendicular to the external field \mathbf{B} and thus responding the most sensitively to the latter.

We can now estimate roughly the value of the density of the vortices contributing to the diamagnetic response in the temperature range of interest. Using the above values of E_0 and n_0 and taking into account a reduction factor of 0.15 (see below), we get $n_V \sim 10^2 \mu\text{m}^{-2}$ for $T = 65$ K. This relatively small value will be discussed in the next section but we should not forget the fact that it concerns only the part of the total number of vortices that contains elements perpendicular to the layers. We also remark that $\sqrt{n_V^{-1}} \gg a$, which fully justifies the continuous approach in the lattice planes used in the LD action (1).

B. Field dependence of the magnetization

Here we have to deal with coexisting thermal loops and field-induced vortex lines. The magnetic-field dependence in expression (23) for χ is hidden in the density n_V and, possibly, in $n_3 d$, the interplanar correlation length. The most simple approach to deal with this situation consists in splitting n_V into a thermal and a field-induced part as follows:

$$n_V = n_V^{th} + n_V^f \equiv n_V^{th} [1 + z(T, B)]. \quad (26)$$

This gives naturally rise to the dimensionless variable

$$z = \frac{n_V^f}{n_V^{th}} = \frac{B}{\Phi_0 n_V^{th}}, \quad (27)$$

quantifying the relative importance of the two types of vortex elements. Assuming that n_3 does not depend on B , one can integrate $\chi(T, B)$ in order to obtain the magnetization per unit volume,

$$M(T, B) = -\frac{1}{(1+2n_3)d} \frac{k_B T}{\Phi_0^2} [\Phi_0 \ln\{1+z(T, B)\} + (\pi\gamma)^2 n_3 (1+n_3) d^2 B]. \quad (28)$$

The corresponding molar quantity is multiplied by the additional prefactor $\lambda \Omega_M$ already mentioned at the beginning of this section. M depends on temperature through n_V^{th} and, possibly, through n_3 . The first contribution to Eq. (28), given by $\ln(1+z)$, has two different limiting behaviors. For low fields $\ln(1+z) \sim z$ and M is essentially given by $\chi(T, B=0)B$, whereas for high fields the first part of M varies like $\ln(z)$. The crossover between the two regimes takes place for $z \sim 1$ that describes the situation where the quantities of thermally excited and field-induced vortex-line elements are similar to one another. Thus the corresponding field value depends crucially on the thermal vortex element density n_V^{th}

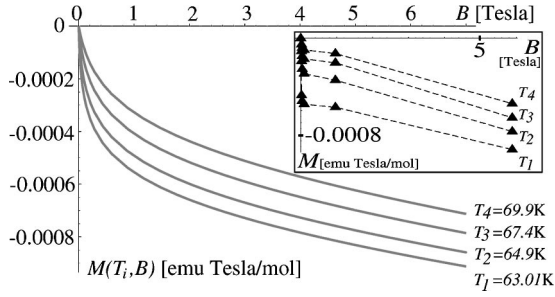


FIG. 3. Magnetization $M(T=\text{const}, B)$: the full lines correspond to the theoretical expression (28) with the values of the parameters mentioned in the text and the triangles (\blacktriangle) in the inset are the experimental data from Ref. 6.

showing up in the dimensionless variable z defined in Eq. (27). Using the values obtained in Sec. III A for the parameters n_0 and E_0 entering n_V^{ih} , and choosing λ such that the theoretical curves and the experimental data match reasonably, we find that $z \sim 1$ corresponds to a field $B_c \sim 0.025$ T. This is shown on Fig. 3 where we note that the experimentally observed behavior shows indeed a crossover at fields of the order of 0.05 T. Therefore our theoretical crossover field B_c is a bit too small. However the two different regimes observed experimentally can be clearly interpreted in the framework of our theory: they describe the two situations where the diamagnetic response is essentially due to solely one type of vortex-line elements (thermal for small B and field induced for large B). This is already gratifying for a first approach. For larger fields the term $\ln(z)$ would yield a magnetization that increases more slowly with B than the measured data, which rather show a linear B dependence. This is reproduced by the second part of Eq. (28) that, in our procedure, arises from the vortex correlations between different layers and becomes relevant for large values of B .

These considerations are illustrated on Fig. 3 where the data from Ref. 6 are shown together with the theoretical curves given by Eq. (28). Although the quantitative agreement is less spectacular than in the case of the zero-field susceptibility, it still allows to extract the values of the ‘magnetically active volume fraction’ λ (from the small B region) and of the anisotropy parameter γ (from the large B region). For the four temperatures of interest we find that the choice $\lambda \sim 0.15$ is the most satisfying. This is quite reasonable for a layered compound such as underdoped YBCO where superconductivity occurs only in copper oxide planes that represent only a small fraction of the unit cell. Concerning the anisotropy γ , we find a value ~ 2 . Its order of magnitude is correct since, by multiplying it by the lattice anisotropy $d/a \sim 3$, we obtain a value of 6 for the effective anisotropy. The latter is somewhat lower than what is observed in penetration-depth measurements where it is found to be of the order of 25 at T_c .¹⁶ However, we recall that γ entered our theory through the vortex line effective stiffness in Eq. (20). This rather rough description of the vortex loops interlayer correlations and the assumption we made by keeping n_3 independent of the temperature may possibly explain the fact that the observed value is a bit different from 25. Using the values of λ and γ discussed above, it is now

possible to show that the second term in our expressions (23) and (28) is irrelevant for the low-field behavior, as we have anticipated when fitting the zero-field susceptibility. Finally we note that the picture of the vortex structure emerging from the above analysis that consists in loops and lines losing their interplanar correlations over a very short distance $n_3 d$ agrees very well with the usual descriptions of a vortex system at temperatures lying above T_c and above the vortex melting and a possible vortex-decoupling line.^{8,10,26–29}

However, as Fig. 3 shows, the experimentally observed crossover is extremely sharp—in fact much sharper than what we can obtain using our expression (28). This observation calls for a more refined treatment where other effects of the magnetic field than the mere creation of vortex lines must be taken into account.

It is in fact possible to understand, in the framework of our approach, what makes the crossover so sharp. In terms of the susceptibility $\chi(T, B)$ in Eq. (23), the sharpness of the crossover suggests that the first term must tend to zero very rapidly as B increases. In this way, only the second (approximately constant) term remains and then yields the linear behavior of the magnetization $M(T, B)$ for $B > B_c$.

This behavior could be achieved by assuming a small magnetic-field dependence of the activation energy E_0 and be motivated as follows. In Ref. 21 it is emphasized that, below T_c , the effective interaction between vortex loops is screened by the thermal defects of the Abrikosov vortex lattice. For small B , this effect is enhanced when the magnetic field is increased because the density of vortex lines is directly proportional to B as in Eq. (27). Above a crossover field B^* the screening becomes weaker due to the fact that the finite stiffness ($\propto B^2$) of the vortex lines inhibits the formation of further defects. In the liquid phase above T_c that we are interested in, a similar qualitative behavior can be expected, at least for low fields. A screened interaction between vortex loops then reduces the energetic cost of creating such an object. Thus the total number of thermally excited vortex loops must increase with the magnetic field B . Among them a (small) percentage corresponds to those contributing to the diamagnetic response as discussed in the previous section. They will also follow the above behavior so that we may reasonably assume that their effective activation energy E_0 introduced in Eq. (25) must decrease slightly when the magnetic field B increases. To lowest order, we have

$$E_0 \rightarrow E_0(B) = \begin{cases} E_0(1 - \alpha B), & B \ll B_c \\ E_1 < E_0, & B \gg B_c. \end{cases} \quad (29)$$

The large B behavior is not important since it affects only the first term of the susceptibility when it is already very small. To illustrate this idea, we take $\alpha = 1$ such that the value of the activation energy saturates at a value E_1 , 20% lower than E_0 around $B = 0.5$ T. After having performed a numerical integration of the susceptibility $\chi(T, B)$ over B , we obtain the curves shown in Fig. 4. The crossover between the two-field regimes is sharper than in the previous case and the corresponding value of the magnetic field B_c is higher.

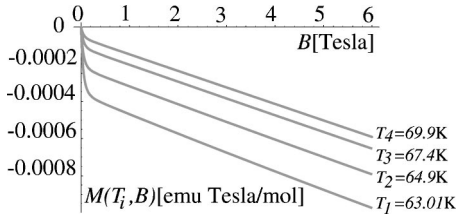


FIG. 4. Improved version of the magnetization $M(T = \text{const}, B)$: the full lines correspond to the theoretical expression based on Eq. (29).

We emphasize however that the above strategy was only intended to show how the developed formalism could be modified in order to improve the interpretation of the experimental results from Ref. 6. A proper justification of the above assumption (29) requires concepts and methods that are beyond the scope of this work.

IV. SUMMARY AND CONCLUSIONS

We have derived explicit expressions for the field- and temperature-dependent diamagnetic susceptibility $\chi(T, B)$ and magnetization $M(T, B)$ of an anisotropic superconductor above its critical temperature. The superconducting fluctuations above T_c are treated in the framework of the Lawrence-Doniach model including a magnetic field \mathbf{B} perpendicular to the lattice planes. In order to describe specifically the precursor effects above T_c , we have used the London approximation, assuming thereby that the relevant fluctuations are given by the phase of the order parameter only. Such an approach should apply to the underdoped regime of cuprates. In this context the current-current correlation function that determines χ and M is expressed by the structure factor of the relevant phase excitations—the thermally excited vortex loops and the field-induced vortex lines. Our expressions for χ and M contain still several undetermined parameters such as the areal density of vortex-line elements within a given layer, an appropriate length describing vortex-line correlations between different layers, the anisotropy, and a factor smaller than one that gives the fraction of the volume of the superconductor that is “active” in contributing to the fluctuation induced diamagnetism. These quantities, which must be compatible to another, are estimated by comparing $\chi(T, B=0)$ and $M(T, B)$ to experimental data obtained on underdoped YBCO⁶ and allow then to deduce an accurate picture of the phase system of such materials. Our findings can be summarized as follows.

(i) There have been attempts to understand the same data based on Gaussian fluctuations of the anisotropic LD model.⁶ The corresponding fit for optimally doped YBCO, where the precursor region is much narrower, has worked out successfully. However, the discrepancies between experiment and the corresponding theoretical curves for the underdoped compound are very large, both in the temperature and magnetic-field dependences. Our approach, based on topological phase excitations in a noncritical regime, is much more satisfactory.

(ii) The experimental low-field susceptibility has an acti-

vated temperature behavior. This observation indeed points to excitations that have a finite creation energy (the vortex loops), rather than some wavelike fluctuations of the pairing field (the Gaussian modes). The value of the activation energy is roughly 20 times the critical temperature, which shows that the relevant vortex loops extend over several layers. The density of those loops is relatively small, indicating that, close to the critical temperature, the phase system consists predominantly of vortex loops running essentially parallel to the planes, and the line elements in z direction that contribute to χ only develop significantly above the critical temperature.

(iii) The interlayer current correlations reflecting the geometrical structure of vortex loops in the z direction are taken into account in terms of an effective correlation length $\xi_3 = n_3 d$. The value of the latter has been determined by the vortex-loop activation energy. In the temperature range of the measurements it is small, typically 2 or 3 interlayer distances. This feature can be also characterized by the stiffness of the vortex line that is found to be approximately inversely proportional to the anisotropy parameter. These observations indicate that the observed phase structure corresponds very well to the picture of weakly coupled layers of two-dimensional “pancake” vortices.

(iv) In the calculation of the molar susceptibility we have multiplied the molar volume by an overall prefactor called “effective active volume fraction” taking into account only those parts of the unit cell that contribute to superconducting fluctuations. This quantity was found to be of the order of 10–20%.

(v) Both the activated behavior of χ and the small value of the above correlation length $\xi_3 = n_3 d$ point to the fact that the measurements of Ref. 6 cover a “precritical” regime. Indeed, although the relevant physics is governed by phase fluctuations according to our assumptions, no divergence of the 3D XY type has been observed. The latter is nevertheless expected for the data taken the closest to T_c , as it has been identified in Ref. 8 for layered superconductors with a reasonable value of the anisotropy. In fact one observes that some deviations from the activated behavior appear for the temperatures closest to T_c . This may indicate a crossover to a critical regime in which the T dependence of χ is no more simply governed by the *total* vortex density, but by a diverging correlation length ξ associated with the *free* vortex density that should be used instead of n_V in the structure factor (14) and in χ [Eq.(23)], as it was done in the 2D case for calculating the zero-field susceptibility.¹⁵ Moreover, in this case the dimensionless quantity z defined in Eq. (27) becomes the scaling variable $B\xi^2/\Phi_0$ that has been used extensively to study critical properties under magnetic field.¹⁶

(vi) The experimental data show an extremely sharp crossover in the field dependence of the magnetization. Within our approach this is attributed to a subtle interplay between the two types of vortices suggesting that the presence of field-induced vortex lines is favoring the creation of thermal vortex loops containing at least two segments along the z direction. However, even our most refined theoretical curves are still more smooth than the data. It is therefore not excluded that the observed behavior may have yet another

origin than superconducting fluctuations, for instance sample inhomogeneities, as it has been suggested and observed in other samples by the authors of the experimental work⁶ that we have analyzed.

ACKNOWLEDGMENTS

We thank X. Zotos, A.A. Varlamov, S.R. Shenoy, and T. Schneider for interesting discussions. This work has been supported by the Swiss National Science Foundation (Projects Nos. 20-49586.96 and 2000-053697.98/1).

APPENDIX

Here we show that the zero-wave vector value of the positional structure factor (12) compensates the singular term of the current-current correlation function (11). Starting from Eq. (12), we find

$$\begin{aligned} S(\mathbf{q}=0) &= \sum_{n,s,n',s'} t(s,n)t(s',n') \\ &= \sum_{n,n'} (N_+ - N_-)^2, \end{aligned} \quad (\text{A1})$$

where N_+ [N_-] is the number of vortex-line elements with $t(s,n) = +1$ [$t(s,n) = -1$] in layer n . They correspond exactly to the 2D concepts of vortex and antivortex that are often interpreted as positive and negative charges of a 2D Coulomb gas.

The external flux generates N_F ‘‘charges’’ according to

$$N_F = \frac{L^2 B}{\Phi_0}. \quad (\text{A2})$$

Due to the incompressibility of the magnetic field ($\nabla \cdot \mathbf{B} = 0$), this number is the same for all layers.

The neutrality condition requires that, in every layer n , the external flux is exactly compensated by the net charge $N_+ - N_-$ of the vortex-antivortex system

$$N_F = N_+ - N_-, \quad \forall n. \quad (\text{A3})$$

Therefore Eq. (A1) may be written as

$$S(\mathbf{q}=0) = N^2 \left(\frac{L^2 B}{\Phi_0} \right)^2, \quad (\text{A4})$$

which is exactly the singular term of the current-current correlation function $C(\mathbf{q})$.

-
- ¹For recent reviews see, e.g., T. Timusk and B. Statt, *Rep. Prog. Phys.* **62**, 61 (1999); J.L. Tallon and J.W. Loram, *Physica C* **349**, 53 (2001).
- ²A. Junod, A. Erb, and Ch. Renner, *Physica C* **317-318**, 333 (1999).
- ³V. Pasler, P. Schweiss, Ch. Meingast, B. Obst, H. Wühl, A.I. Rykov, and S. Tajima, *Phys. Rev. Lett.* **81**, 1094 (1998); Ch. Meingast, V. Pasler, P. Nagel, A. Rykov, S. Tajima, and P. Olsson, *ibid.* **86**, 1606 (2001).
- ⁴A. Schmid, *Phys. Rev.* **180**, 527 (1969); R.E. Prange, *Phys. Rev. B* **1**, 2349 (1970).
- ⁵C. Baraduc, A. Buzdin, J.-Y. Henry, J.-P. Brison, and L. Puech, *Physica C* **248**, 138 (1995).
- ⁶P. Carretta, A. Lascialfari, A. Rigamonti, A. Rosso, and A. Varlamov, *Physica B* **259**, 536 (1999); *Int. J. Mod. Phys. B* **13**, 1123 (1999); *Phys. Rev. B* **61**, 12 420 (2000).
- ⁷V.J. Emery and S.A. Kivelson, *Nature (London)* **374**, 434 (1995); J. Corson, R. Mallozzi, J. Orenstein, J.N. Eckstein, and I. Bozovic, *ibid.* **398**, 221 (1999).
- ⁸B. Chattopadhyay and S.R. Shenoy, *Phys. Rev. Lett.* **72**, 400 (1994).
- ⁹B. Chattopadhyay, M.C. Mahato, and S.R. Shenoy, *Phys. Rev. B* **47**, 15 159 (1993).
- ¹⁰G. Blatter, M.V. Feigel'man, V.B. Geshkenbein, A.I. Larkin, and V.M. Vinokur, *Rev. Mod. Phys.* **66**, 1125 (1994).
- ¹¹Z. Tešanović, *Phys. Rev. B* **59**, 6449 (1999).
- ¹²N.H. March and M.P. Tosi, *Atomic Dynamics of Liquids* (Wiley, New York, 1976), Chap. 7.
- ¹³R. Côté and A. Griffin, *Phys. Rev. B* **34**, 6240 (1986).
- ¹⁴H.J. Kwon and A.T. Dorsey, *Phys. Rev. B* **59**, 6438 (1999).
- ¹⁵B.I. Halperin and D.R. Nelson, *J. Low Temp. Phys.* **36**, 599 (1979).
- ¹⁶T. Schneider and J. M. Singer, *Phase Transition Approach to High Temperature Superconductivity* (Imperial College Press, London, 2000).
- ¹⁷S. Sengupta, P. Nielaba, and K. Binder, *Europhys. Lett.* **50**, 668 (2000).
- ¹⁸G. Kohring, R.E. Shrock, and P. Wills, *Phys. Rev. Lett.* **57**, 1358 (1986).
- ¹⁹J. Epiney, Diploma thesis, ETH Zürich, 1990.
- ²⁰W. Janke and T. Matsui, *Phys. Rev. B* **42**, 10 673 (1990).
- ²¹A. Schmidt and T. Schneider, *Z. Phys. B: Condens. Matter* **87**, 265 (1992).
- ²²G. Carneiro, R. Cavalcanti, and A. Gartner, *Phys. Rev. B* **47**, 5263 (1993).
- ²³A. Tanner, Ph.D. thesis, University of Zürich, 1994.
- ²⁴A.K. Nguyen, A. Sudbø, and R.E. Hetzel, *Phys. Rev. Lett.* **77**, 1592 (1996).
- ²⁵X. Hu, S. Miyashita, and M. Tachiki, *Phys. Rev. Lett.* **79**, 3498 (1997); *Phys. Rev. B* **58**, 3438 (1998).
- ²⁶S. Ryu and D. Stroud, *Phys. Rev. B* **54**, 1320 (1996).
- ²⁷S.-K. Ching, A.K. Nguyen, and A. Sudbø, *Phys. Rev. B* **59**, 14 017 (1999).
- ²⁸M.J.W. Dodgson, V.B. Geshkenbein, and G. Blatter, *Physica B* **280**, 220 (2000).
- ²⁹X.G. Qiu, V.V. Moshchalkov, and J. Karpinski, *Phys. Rev. B* **62**, 4119 (2000).